ELSEVIER

Journal of Nuclear Materials 283–287 (2000) 470–473

journal of nuclear materials

www.elsevier.nl/locate/jnucmat

Effects of helium implantation on hardness of pure iron and a reduced activation ferritic–martensitic steel

Hiroyasu Tanigawa [a,*], Shiro Jitsukawa [a], Akimichi Hishinuma [a], Masami Ando [b], Yutai Katoh [b], Akira Kohyama [b], Takeo Iwai [c]

[a] *Japan Atomic Energy Research Institute, Tokai, Ibaraki 319-1195, Japan*
[b] *Institute of Advanced Energy, Kyoto University, Gokasho, Uji, Kyoto 611-0011, Japan*
[c] *Research Center for Nuclear Science and Technology, University of Tokyo, Tokai, Ibaraki 319-1106, Japan*

Abstract

Helium was implanted into high purity Fe and F82H at room temperature up to 2000 appm to investigate helium effects on hardening. Ultra micro-indentation tests were performed on the specimens before and after helium implantation with loads that penetrate in 300 nm depth. After the indentation tests, the specimens were prepared with a focused ion beam (FIB) processing system for transmission electron microscopy (TEM) of the deformed regions. Results of the indentation tests indicated clearly that helium implantation caused hardening for both pure Fe and F82H. For pure Fe, it was also observed by TEM that the propagation of the plastic deformation zone formed during the indentation was limited to the helium-implanted layer, ranging from 600 to 800 nm from the incident surface.

1. Introduction

A reduced activation ferritic–martensitic steel, F82H (Fe–8Cr–2W–V–Ta), is one of the candidates for the first wall and blanket structural material for a D-T fusion reactor. It has been reported that transmutation-produced helium atoms from (n, α) reactions may play a significant role in the irradiation embrittlement of the alloy during service. There are only a few ways to implant helium into a material, and helium ion implantation using an ion accelerator is the most convenient and accurate method. The main disadvantage of this method is that the helium-implanted region is limited to a few micrometers from the irradiation surface. Because of this, it is generally recognized that helium implantation is not suitable to study mechanical properties. The only way to investigate the mechanical properties of such a small volume is by ultra micro-indentation techniques. Ultra micro-indentation techniques have been developed recently, mainly to measure the mechanical properties of hard thin films on a substrate [1,2] or ion-implanted materials' surfaces [3]. This micro-indentation technique has also been applied to ion-irradiated materials [4–6]. In the current study, the effects of helium on irradiation hardening and embrittlement were investigated by a ultra micro-indentation technique and by microstructural observations in the deformed region.

2. Experimental

The materials used in this study were high purity iron and F82H. The impurity content (P, C, S, O, N, B) of the high purity iron was less than a few appm. A detailed description of F82H composition has been published elsewhere [7]. TEM disks were punched out from sheets of the materials, and polished by the following series: SiC paper up to #4000, 9 and 3 μm diamond powder, 0.3 and 0.05 μm alumina powder, then finished by a electrolytic surface finish.

The helium ion implantation experiment was carried out at the High-fluence Irradiation Facility, University

* Corresponding author. Tel.: +81-29 282 6551; fax: +81-29 282 5922.
E-mail address: tanigawa@realab01.tokai.jaeri.go.jp (H. Tanigawa).

0022-3115/00/$ - see front matter
PII: S0022-3115(00)00085-4

of Tokyo (HIT Facility) [8]. 1 MeV He^+ ions were degraded to 203 and 317 keV to implant helium into a wider range than single energy ion implantation. The profile of the implanted helium was calculated with the TRIM code and the results suggest that the helium ions were implanted to a depth between 600 and 800 nm from the incident beam surface.

Ultra micro-indentation was performed using a UMIS-2000 from CSIRO, Australia, with Berkovich-type tips. Measurements were made at loads to penetrate 300 nm, i.e., 6 mN for pure Fe and 10 mN for F82H. Typically, indentations of the samples were made using a 5×5 array of indents with a 20 μm interval. The results were analyzed in the manner outlined by Oliver and Pharr [9] with further refinements proposed by Mencik and Swain [10].

Hardness, H, is defined as

$$H = P/A(h_c),$$

where P is the indentation load and A, which is a function of contact depth (h_c), is the projected area of contact between the indenter and the specimen. Contact depth is defined as

$$h_c = h_t - 0.75P/(C - C_m) + h_i,$$

where h_t is the total depth, C the compliance measured from the unloading curve, C_m the machine compliance and h_i is the initial contact depth. $A(h_c)$ and C_m were defined by measuring the elastic modulus of fused silica with a variety of load conditions, assuming that the elastic modulus is constant at any depth. UMIS-2000 defined the specimen surface by measuring contact force (e.g. 5 μN in this study) during the initial tip lowering process. Then the initial contact depth was determined by extrapolating a regression of the load–depth curve to zero load.

For the FIB processing, the implanted surface of a TEM disk was covered with hard adhesive and then the disk was nickel-plated on the non-implanted side. A 300 μm thick sheet was sliced in the direction vertical to the disk surface. A half moon TEM disk was drilled out from the sheet using an abrasive slurry disk cutter made

Table 1
Statistic data of hardness for each condition

Materials	Pure Fe				F82H			
He (appm)	0	10	500	2000	0	10	500	2000
Data points	16	20	25	19	15	19	20	20
Average hardness (Gpa)	2.05	2.62	2.53	2.61	3.55	3.43	3.68	3.71
Standard dispersion (Gpa)	0.13	0.05	0.09	0.17	0.18	0.16	0.15	0.25

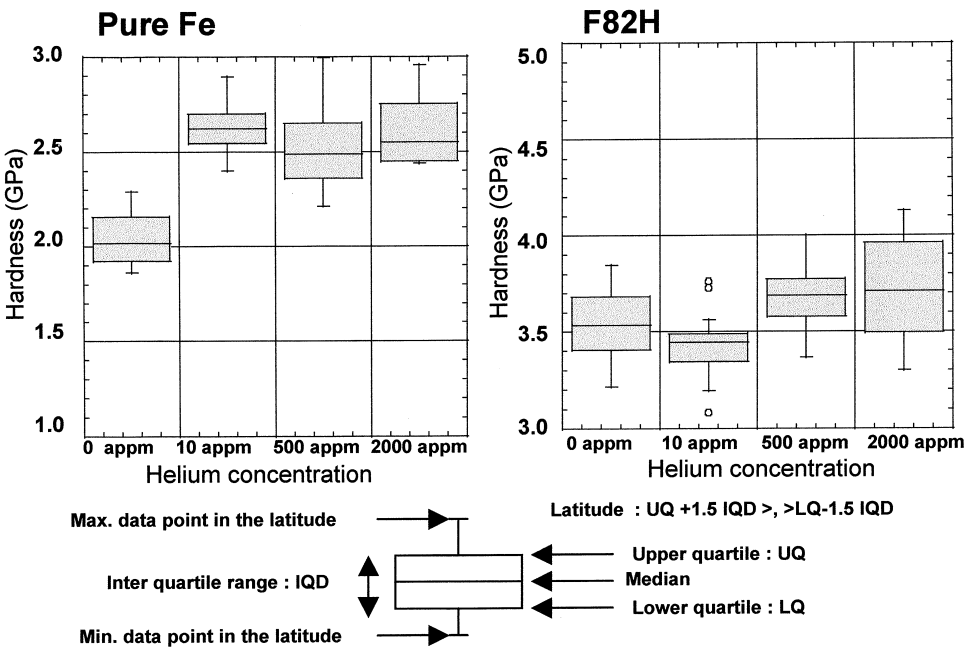

Fig. 1. Hardness dispersion for each condition.

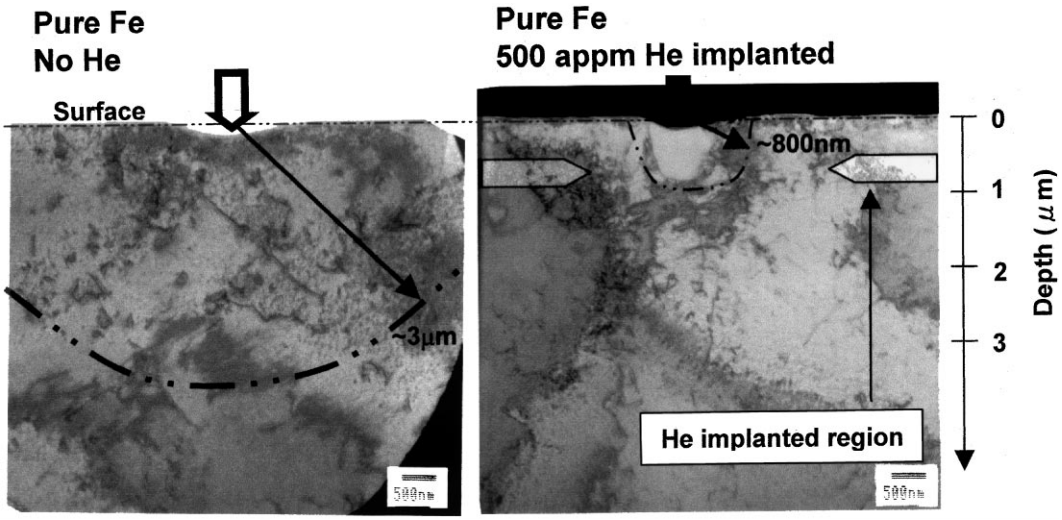

Fig. 2. Bright field images of the region beneath the impression.

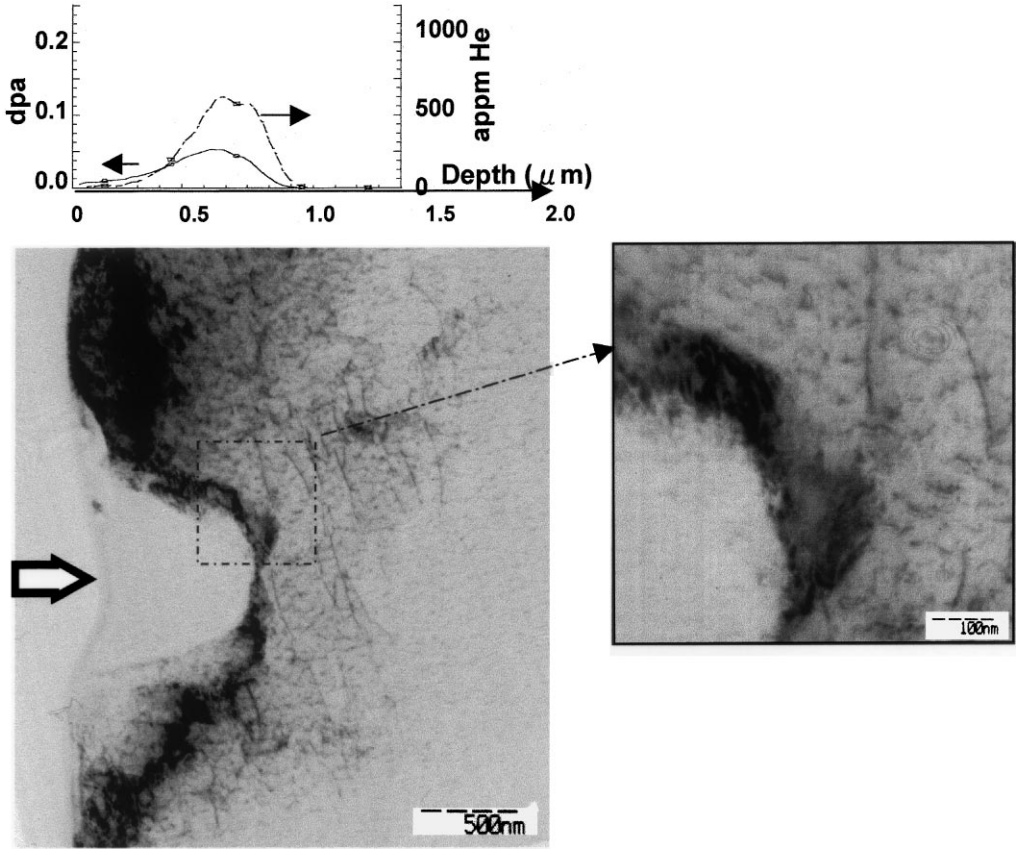

Fig. 3. Dark field TEM image of the region beneath the impression in the helium-implanted Fe. Gradations of images were inverted for more sharp contrast.

by South Bay Technology, and the half moon disk was polished down to 100 μm thick. At last, the adhesive cover was removed by acetone, then indentation tests were performed on the. The thin foil around the impression was made so that they include the indentation axis by means of FIB micro-processing, using Hitachi FB-2000a focused ion beam system. The details of the FIB micro-processing procedure has been explained elsewhere [11]. Microstructure examination was carried out using a Hitachi HF-2000 transmission electron microscope operating at 200 kV.

3. Results and discussion

Table 1 and Fig. 1 show the statistical data and the dispersion of measured hardness, respectively. For pure Fe, about 27 % of hardening compared to the non-irradiated specimen were measured for the helium-implanted specimens, and the degree of hardening was not dependent on the helium concentration. These hardening were the results of helium implantation, but it should be noted that the radiation damage induced by 10,500 and 2000 appm implanted helium were up to 0.001, 0.05 and 0.2 dpa at the peak, respectively. It is shown in the literature that the radiation damage in this range can produce significant hardening in pure Fe [12,13]. Therefore, it must be noted that the hardening in pure Fe shown here could contain the effect of radiation damage.

For F82H, no hardening was measured for the 10 appm helium-implanted specimen, and a little hardening (about 4%) was measured for 500 and 2000 appm He. Both results suggest that helium implantation generally causes hardening for both materials. It may be that the helium hardening effect was small compared to the hardness of the unimplanted material.

Bright field TEM images of the region beneath the impression are shown in Fig. 2. For pure Fe, induced plastic deformation zone was about 3 μm deep, whereas the maximum indenter depth was about 300 nm. That is, the plastic zone was 10 times the size of the indentation depth. On the other hand, the plastic deformation zone was clearly limited to 800 nm from the center of the impression for the 500 appm helium-implanted Fe. Fig. 3 shows the dark field TEM image of the region beneath the impression in the 500 appm helium-implanted Fe. Here, it is clear that the plastic deformation zone was completely terminated at the helium-implanted region, and also terminated at the region near the surface, where the helium concentration was less than 10 appm. This result suggests that dislocation movement was blocked by helium, probably strongly combined with vacancies, and even less than 10 appm helium would be enough for the obstruction. Also, grain boundary-like contrast was observed between the strongly deformed zone and the undeformed zone. With this specimen, the microstructure around this boundary is too complicated to analyze the details. The observation of the microstructure around the impression by lower load should be done for more detailed analysis in the future.

4. Summary

Ultra micro-indentation tests were performed on helium-implanted pure Fe and F82H, and microstructure below the impression in pure Fe and that with 500 appm He were examined by means of FIB processing and TEM observation. The following are the main results of the present work:

1. Helium implantation caused hardening in both materials. About 27% of hardening was observed for any appm helium-implanted pure Fe and about 4% of hardening for over 500 appm helium-implanted F82H.
2. For 10 appm helium-implanted F82H, no hardening was detected, suggesting the possibility that the helium hardening effect was small for the more complex microstructure of F82H.
3. The plastic deformation zone of the 500 appm helium-implanted pure Fe specimen was clearly terminated at the helium-implanted region; 600–800 nm depth from the incident beam surface.
4. The propagation of the plastic deformation zone of the 500 appm helium-implanted pure Fe specimen was also limited to a shallower region with <10 appm implanted helium.

References

[1] N.G. Chechenin, J. Bottiger, J.P. Krog, Thin Solid Films 261 (1995) 219.
[2] M. Wittling, A. Bendavid, P.J. Martin, M.V. Swain, Thin Solid Films 270 (1995) 283.
[3] R. Nowak, C.L. Li, M.V. Swain, Mater. Sci. Eng. A253 (1998) 167.
[4] S.J. Zinkle, W.C. Oliver, J. Nucl. Mater. 141–143 (1986) 548.
[5] P.M. Rice, R.E. Stoller, B.N. Lucus, W.C. Oliver, Proc. Mater. Res. Soc. Symp. 373 (1995) 205.
[6] Y. Katoh, H. Tanigawa, T. Muroga, T. Iwai, A. Kohyama, J. Nucl. Mater. 271&272 (1999) 115.
[7] K. Shiba, M. Suzuki, A. Hishinuma, J. Nucl. Mater. 233–237 (1996) 309.
[8] Y. Kohno, K. Asano, A. Kohyama, K. Hasegawa, N. Igata, J. Nucl. Mater. 141–143 (1986) 794.
[9] W.D. Oliver, G.M. Pharr, J. Mater. Res. 7 (1992) 1564.
[10] J. Mencik, M.V. Swain, Mater. Forum 18 (1994) 277.
[11] M. Ando, Y. Katoh, H. Tanigawa, A. Kohyama, J. Nucl. Mater. 271&272 (1999) 111.
[12] B.N. Singh, A. Horsewell, P. Toft, J. Nucl. Mater. 271&272 (1999) 97.
[13] Y. Chen, P. Spätig, M. Victoria, J. Nucl. Mater. 271&272 (1991) 128.